Research on Microstructure and Growth Model of C/C Composites by Chemical Vapor Infiltration

Zhiyong Xie, Qizhong Huang, Cailiu Yin, Lihai Liu, Mingyu Zhang, Zhean Su,
Xiufei Wan , Boyun Huang
State Key Laboratory of Powder Metallurgy, Central South University, Changsha 410083, China

Abstract

The self-designed infiltration reactor with coupling physical fields was applied to fabricate Carbon/Carbon composites. A special conductive layer was installed in the preforms to generate strong electromagnetic and thermal gradients. A carbon fiber felt with the size of 260 mm×60 mm×20 mm was infiltrated at temperatures of 1200 K to 1400 K and furnace pressure from 3 to 15kPa to explore new method and to gain an understanding of the infiltration mechanisms. The texture and microstructure of the infiltrated carbon was studied by polarized-light microscopy, XRD, SEM and laser Raman spectra respectively. The results show that C/C composites with bulk density of 1.71g/cm3 can be obtained in 20h and the ratio of precursor utilization exceeds 20%. A pure, high-textured carbon matrix is formed in the pressure about 4 kPa at 1270K. At higher temperature, a lower textured banded structure is formed, but a higher-textured carbon micro-tree is detected. Meanwhile, high-structure can be obtained in a wider parameter range due to the effect of electromagnetic field. At last, the growth model of pyrolytic carbon was presented to well describe the deposition mechanisms.

Key words

Chemical vapor infiltration; Carbon composites; Pyrolytic carbon

1. Introduction

The chemical vapor infiltration (CVI) is a key method in preparing high performance Carbon /Carbon (C/C) composites, which is two-factor structure including carbon fiber and pyrolytic carbon. The performance of the composites is influenced by the microstructure of pyrocarbon and the fiber weave patterns, but the type of microstructure is examined first. Hence, many efforts have been taken to study the growth of pyrocarbon. It is generally accepted that there are four types of pyrocarbon, which are rough layer (RL), smooth layer (SL), isotropic carbon (ISO) and band structure. SL is formed at low temperatures and high carbon source partial pressure, whereas RL is deposited in the medium range of these parameters and ISO at high temperature with a rather low pressure. However, there is no evidence that a unique chemical method exists to obtain a definite type of microstructure. The sequences of microstructure could result from a change in the local conditions, out of the control of the external parameters. Being higher texture, RL is consumed most largely, and widely used for aircraft brake disc material due to its better friction and wear property. However, this structure is very difficult to obtain in the CVI process, so it has become a focus for the study of C/C composite at present; SL, with better mechanical performances, is mainly used as high temperature structural material and anti-ablation material, which is easier to obtain; ISO structure, with its better isotropy, biocompatibility and densification, is generally used in semi-conductor material, biomaterial and seal material, but it is more difficult to obtain.

The pyrocarbon microstructures vary greatly due to different process conditions or furnace conditions, and it could be decided by its growth model. In this paper, pyrocarbon was prepared by a method called multi-factor coupling physical fields CVI, and the microstructures of pyrocarbon were characterized by Polarized Light Microscopy (PLM), X-Ray Diffraction (XRD), Raman Spectrum and Scan Electron Microscopy (SEM) respectively, and then the two typical growth models of pyrocarbon was studied.

2. Experiments

Carbon felt was used as enforcement, the original density of perform was 0.2-0.4 g/cm^3, and the size of perform was 260 mm×60 mm×20 mm. We installed special shaped conductive layers into the inner or the surface of the preform, and then fabricated C/C composites by self-made multi-factor coupling physical fields CVI reactor. The petroleum liquefaction gas was introduced as carbon source and N_2 as carried gas. The deposition temperature varied from 1200 K to 1400 K, and the furnace pressure from 3 to 15kPa. Carbon source gas content varied from 25% to 75%. All samples were deposited for 20 h and then heat-treated at T=2300℃ for 2 h. The MEF3A polarized-light microscopy (PLM) was applied to determine the texture of pyrocarbon deposited around carbon fibers; The graphitization degree and crystallite size were measured by the X-ray diffraction (XRD) of mean peak position method, the degree of crystallinity and the micro-structural changes were analyzed by Raman Spectrum, and the morphology of fracture surface and deposition surface were observed by scanning electron micrographs (SEM).

3. Results and Discussion

3.1 Polarized optical analysis

Fig.1 shows three polarized-light optical photographs of polished cross-sections. Each type has unique optical characteristics, as described by Pierson and Lieberman. Fig.1(a) exhibits well defined extinction crosses, few discernible growth feature, grey layers, corresponding to smooth laminar (SL) structure; Fig.1(b), in contrast, displays numerous irregular extinction crosses, many growth features, and high optical reflectivity, showing the feature of rough laminar (RL) structure; Fig.1(c) exhibits few, if any, extinction crosses and has low optical reflectivity, amounts of growth cones, at the same time, many trees taper outwards from the deposition surface of pyrolytic carbon, they display the feature of band-structure structures at a certain extent. In addition, the sample (a)'s interfaces of pyrocarbon around the fibers were straighter than the sample (b)'s, and the sample (b)'s were more than the sample (c)'s. It demonstrates that deposition model differs from each other.

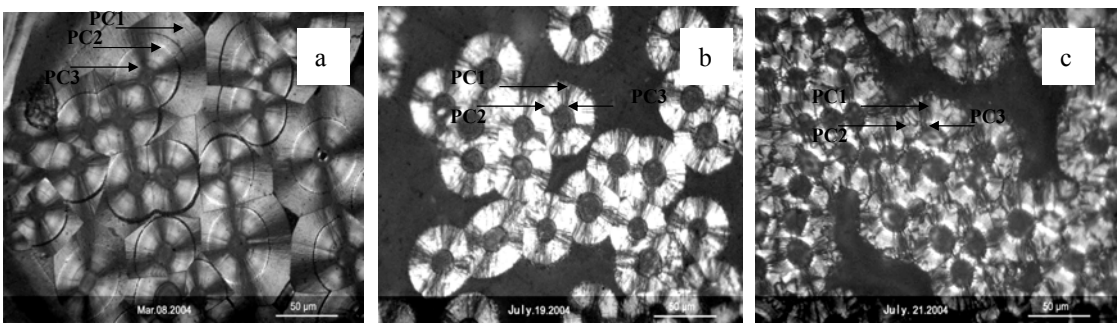

Figure 1. Three typical polarized optical micrographs of samples from the infiltrations; (a) feltⅠ, (b)feltⅡ, (c) feltⅢ, the samples (a), (b), (c) are deposited at a pressure of 4kPa and temperatures of 1220K, 1270K, 1320K, respectively.

3.2 XRD Analysis

Structure parameters of XRD of three kinds of C/C composites were listed in Table 1. XRD measurements were performed with a Rigaku-D/max-3C diffractometer, Si was used as an internal standard and Cu as target, working voltage was 40kv and current 200 mA. According to the mean peak position, the gravity position and the center position of full width of half maximum, three 2θ values were acquired, then according to the function of G=(0.3440-d002)/(0.3440-0.3354)×100%, the value of graphitization degree was calculated, the mean value was used as the graphitization degree. And the mean value of crystallite sizes Lc was calculated according to the Bragg equation.

Table 1. Structure parameters of XRD of three kinds of C/C composites; (a) feltⅠ, (b)feltⅡ, (c) feltⅢ.

Run no.	***2θ*/(º)**	***d002*/nm**	***g*/%**	***Lc*/nm**
a	25.896	0.34210	22.1	7.6
b	26.238	0.33755	75.0	17.4
c	26.127	0.33881	60.3	12.0

After heated treatment at T=2300^{o} for 2h,the graphitization degree of the samples (a), (b) and (c) was about 20%, 75%and 60% respectively. Firstly, the brightness of pyrolytic carbon under the polarized light was an important evidence to judge high textural pyrolytic carbon. The whole pyrolytic carbon of sample (b) appeared silver gray, g >75%. Secondly, the micrography of polarized light was also an important evidence to distinguish sample (a) from sample (c). Although brightness of sample (a) was almost same as sample (c), the graphitization degree was obviously different. For instance, the former was 20%, the value of which approached to a single SL structure, but the later was over 60%, the value of which approached a single RL structure. The main difference between sample (a) and (c) was the roughness of the morphology, and the later is rougher than the former under the polarized light. In addition, the microcrystalline planar size ***La*** of sample (b) was more than sample (a) and (c). This indicates that there exists different deposition mode to illustrate the form of microstructure of pyrocarbon.

3.3 Raman Spectra Analysis

As indicated in Fig. 1, spectra at interior (PC3), center (PC2) and exterior (PC1) of pyrocarbon sheath around a fiber were recorded. Fig.2 shows Raman spectra of pyrolytic carbon in the C/C composites at different deposition ring in different samples. A comparison between PC3, PC2 and PC1 of a pyrocarbon sheath of each sample was carried out to determine the micro-structural changes along axes normal of the sheath around fiber,

which are deposited in different stage. The curves in Fig. 2a, Fig. 2b and Fig. 2c correspond to Fig. 1a, Fig. 1b and Fig. 1c respectively. Fig. 2d is deposition ring dependence of Raman parameter R^{-1} in forementioned samples. The bands of disorder-induced D (1350/cm) and graphite-induced G (1580/cm) can be seen. The ratio of the D to G peak intensity, ID/IG, is inversely proportional to the microcrystalline planar size La , i.e. R^{-1} is proportional to La. It also can be used in the study to determine the degree of graphitization of pyrolytic carbon of micro-zone, and to quantitatively relate microstructure to the process parameters. The sample (a) shows lower values of R^{-1} and less drastic change in R^{-1} in different deposition ring, although the abnormal graphitization occurs in the carbon fiber near the fiber/matrix interface. All values of R^{-1} in Fig.2b are much high, especially in middle ring. This indicates that the deposition micro-circumstance generally changes in infiltration process, which affects the micro-structure of pyrolytic carbon. Fig.2c shows the drastic change of values of R^{-1}. There is abnormally highest value of R^{-1} in the carbon microtrees, much lower in middle and interior ring. The transition is abrupt. The figures reveal a complex relationship between deposition conditions and microstructure, and although at uniform condition, there exists different texture at different deposition term. The results also show higher-textured carbon can be deposited on lower-textured carbon in a reproducible. So, predicting carbon microstructure from temperature and total pressure remains difficult, especially at different micro-zone and deposition term, and detailed investigations may be required on the deposition mechanisms.

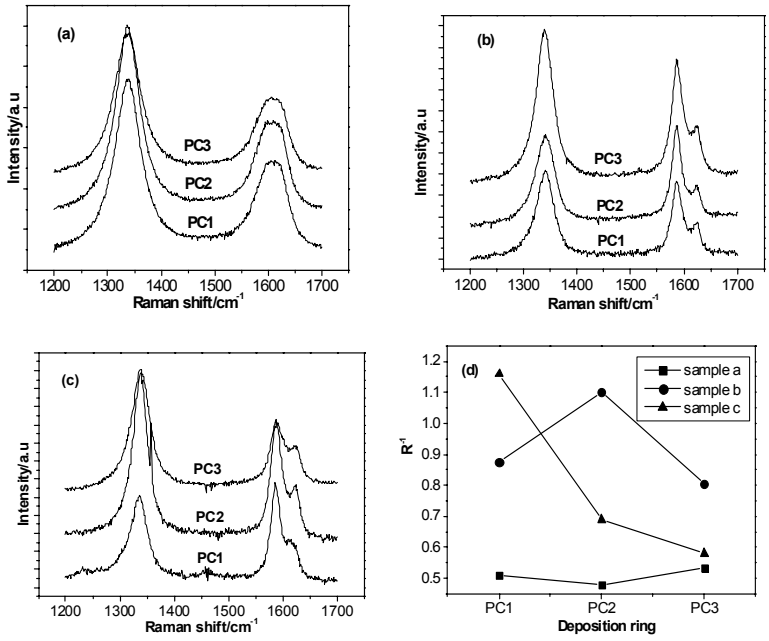

Figure 2. Raman spectras of pyrolytic carbon of different deposition stage around a fibre; (a) feltⅠ, (b)feltⅡ, (c) feltⅢ, (d) changes of Raman parameter R^{-1} of samples (a), (b), (c); PC-pyrocarbon.

3.4 SEM Observations

Fig. 3(a), (b) and (c) showed scanning electron micrographs of fracture surfaces of the pyrocarbon matrix layers resulting from the three-point bending test (corresponding Fig. 1a, 1b and 1c respectively) at the same modification. The fracture surfaces of the matrix of all samples showed characteristic features, i.e. they are not homogeneous indicating different structures of the pyrocarbon. A smooth, flat and compact fracture surface was detected in Fig. 3a. The fracture surface of RL with the laminated structure obviously was rather rough and zig-zag-like, in which the thickness of carbon layer was in a nano-scale (Fig. 3b); Moreover, the fracturing of all

matrix layers occur approximately in the same fracture plane. However, Fig. 3c presented distinctly three fracture plane corresponding with Fig.1c well, but the bright parts of polarized light micrography not obviously appeared zigzag in SEM micrograms.

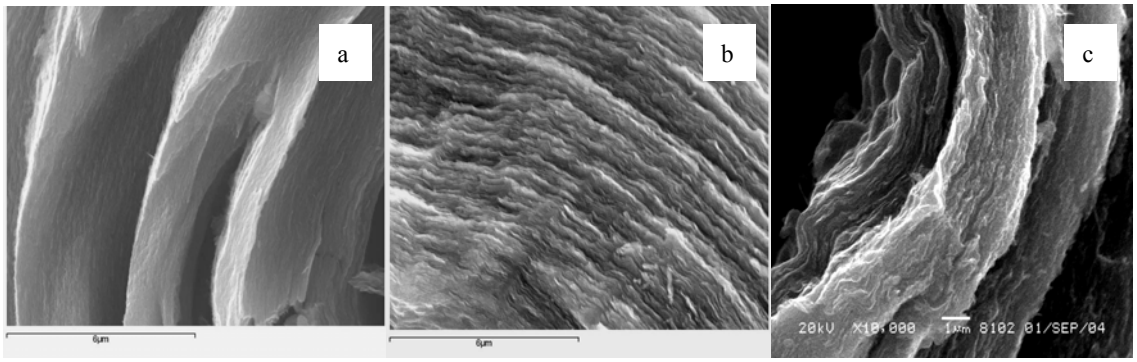

Figure 3. Scanning electron micrographs of fracture surfaces of pyrocarbon matrix layers of the felts obtained in the three-point bending test; (a) feltⅠ, (b)feltⅡ, (c) feltⅢ.

Fig. 4(a)-(c) showed scanning electron micrographs of deposited-surface of pyrocarbon after infiltration at the same modification. The deposition surface of SL was very smooth. However, a lot of convex or granular structure was formed on the surface of RL.

According to SEM observation, the results revealed growth characteristics of different microstructure. SL was formed from smaller molecule, which leaded to forming of small crystallites with higher surface energy. The small crystallites can deposit on surface in a comparatively free and uniform manner. Therefore, the fracture and deposition surfaces of low texture carbon generally were smooth and dense. RL was formed from larger species of laminated structure, and the larger species were firstly stacked on the activation sites of the deposition surface forming growth cones rapidly. More activation sites exist at the edges of grapheme layers. It is important to state that reactive species of any size may react at active sites resulting in extension of carbon plane. These considerations suggest a reinforcement of the tendency of forming laminated structure. To sum up, the results illuminated that the morphologies of fracture surface and deposition surface could be an important evidence to judge the pyrolytic carbon structures.

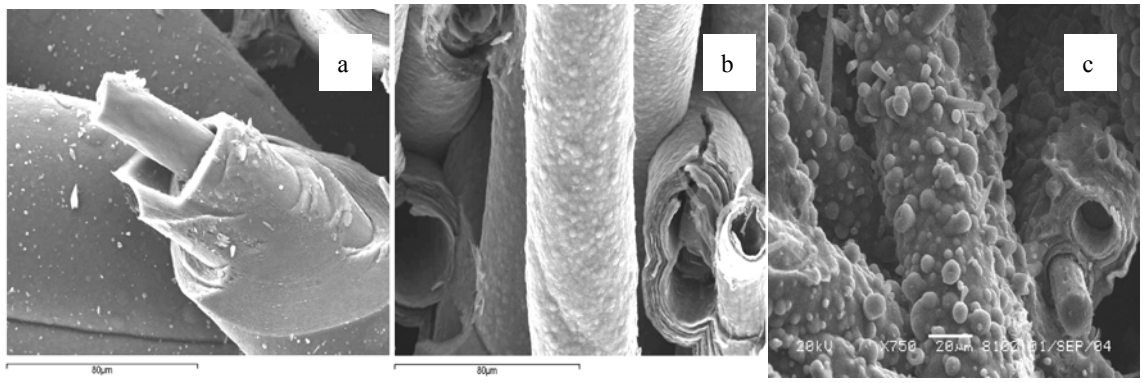

Figure 4. Scanning electron micrographs of deposition surface of pyrocarbon around carbon fiber in C/C composites; (a) feltⅠ, (b)feltⅡ, (c) feltⅢ.

3.5 The Growth Model of Pyrolytic Carbon

The experiment results indicated that the deposition of pyrocarbon could mainly exhibit two growth model, including smoothness growth model and taper growth model. For smoothness growth model, the growth surface presented smooth and homogeneous, and the pyrocarbon interfaces between adjacent fibers were straight, and the pyrocarbon by this model exhibited lower texture and less microcrystalline planar size ***La***, and around the fiber a distinct layer could not be detected showing a rather smooth and compact fracture surface. These results confirmed that the carbon layer was deposited gradually from small hydrocarbon species with a smaller deposition rate. Such a model could illustrate that the final densification rate of this model was fast comparatively. For taper growth model, the growth surfaces presented taper morphology, and the intensity of the taper had a distinct increase with increasing deposition temperature and pressure, which revealed that the high-texture carbon was deposited drastically from large and small hydrocarbon species even forming carbon micro-tree structure. The growth competition directly resulted in the pyrocarbon interfaces between adjacent fibers becoming unclear. Moreover, the pyrocarbon from this model exhibited higher texture and larger microcrystalline planar size ***La*** with the increase of the taper height. However, there is no evidence that a unique chemical method exists to lead to a definite type of growth model, and high-texture pyrocarbon can be deposited on low-texture pyrocarbon in a reproducible manner.

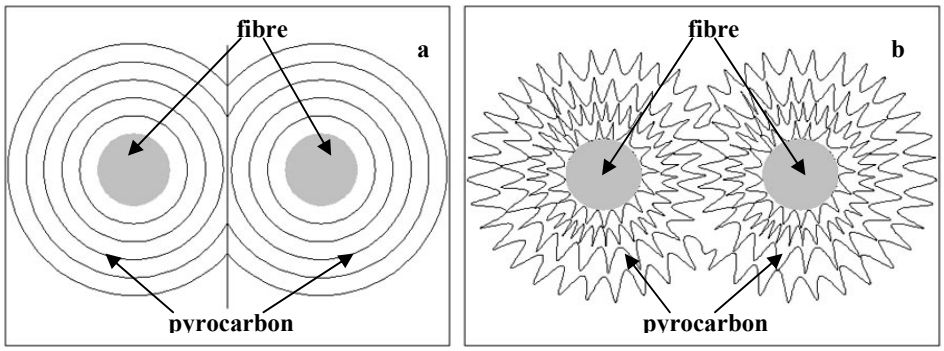

Figure 5. Two typical growth model pyrolytic carbon by CVI

（a）smoothness growth model （b） taper growth model

4. Conclusion

(1) The sequences of (RL-SL-Band structure) microstructures can be found for a given experimental setup called multi-factor coupling physical fields CVI. In addition, the high-textured carbon micro-tree is detected during the infiltration process, in particular during higher deposition temperature.

(2) There exists different texture of pyrocarbon around the same fiber at different deposition stage even under uniform deposition conditions. Moreover, the high-textured carbon micro-tree can be deposited in a reproducible. The experimental results demonstrate that the texture of pyrocarbon is more strongly influenced by the local deposition conditions than by the external parameters.

(3) Two typical growth models of pyrolytic carbon were put forward, which were smoothness growth model and taper growth model. The smoothness growth model could well describe the growth of low texture pyrocarbon, in which the densification rate was rapid and the interfaces of pyrolytic carbon around the fibers were straight; while the taper growth model could well describe the growth of high texture pyrolytic carbon, but the densification rate was slow and the interfaces of pyrolytic carbon around the fibers were interlocked.

Acknowledgement

This research has been carried out in the State Key Laboratory of Powder Metallurgy financed by the National Basic Research Program of China (also called 973 Program) under grant No.2006CB6009001.

References

Agnes Oberlin. 2002. Pyrocarbons. Carbon 40:7-24.

Ajayan PM, Nugent JM, Siegel Rw, Wei B, Kohler-Redlich PH. 2000. Growth of carbon micro-trees. Nature 404:243.

Benzinger w, Hüttinger KJ. 1999. Chemistry and kinetics of chemical vapor infiltration of pyrocarbon – □. Mechanical and structural properties of infiltrated carbon fiber felt. Carbon 37: 1311-1322.

Buckley JD.1988. Carbon-carbon overview. Ceramic bulletin, 67(2): 364.

Buckley JD , Edie DD. 1993. Carbon-Carbon Materials and composites.Park Ridge,NJ:Noyes Publication 12-14.

Delhaes P. 2002. Chemical vapor deposition and infiltration processes of carbon materials. Carbon 40: 641-657.

De Pauw V, Reznik B, et al. 2003. Texture and nanostructure of pyrocarbon layers deposited on planar substrates in a hot-wall reactor. Carbon 41: 71-77.

Fitzer E.1987.The future of carbon-carbon composites. Carbon 25:163.

HU ZJ, Zhang WG, Hüttinger KJ, Reznik B, Gerthsen D. 2003. Influence of pressure, temperature and surface area/volume ratio on the texture of pyrolytic carbon deposited from methane. Carbon 41:749-758.

TANG Zhong-hua,ZHOU Gui-zhi,XIONG Jie,et al. 2003. Measurement of graphitization degree of carbon-carbon composites by average X-ray diffraction angle method. The Chinese journal of nonferrous metals, 13 (6): 1435-1440.

Xie Zhi-yong, Huang Qi-zhong, Su Zhe-an, et al. 2005. Effects of perform density on CVI rate and microstructure of carbon/carbon composites. Journal of Hunan University of Science and Technology 20（2）：41 - 44.

XIE Zhi-yong, HUANG Qi-zhong, SU Zhe-an, et al. 2005. The influence of hydrocarbon gas on the density and microstructure of C/C composites formed by chemical vapor infiltration. New Carbon Materials, 20(2):171-177.

XIE Zhi-yong, HUANG Qi-zhong, SU Zhe-an, et al. 2005. Preparation of C/C composites by CVI with multi-factor coupling physical fields and deposition mechanism. Journal of Inorganic Materials 20（5）：1201 - 1207.

XIE Zhi-yong, HUANG Qi-zhong, SU Zhe-an, et al. 2005. Preparing C/C composites by CVI with multi-factor coupling physical fields and discussing the dynamic process. Acta Material Composites Sinica, 22（4）：47 - 52.

Yung Joon Jung, Bingqing Wei, John Nugent, Pulickel M. Ajayan. 2001. Controlling growth of carbon microtrees. Carbon 39:2195-2201.

Zhang Fu-qin, Huang Bai-yun, Huang Qi-zhong, et al. 2002. Effects of interface on the graphitization of a carbon fiber/pyrolytic carbon composite. Carbon 41: 579-625.

ZHANG W G, Hu Z J, Hüttinger K J. 2002. Chemical vapor infiltration of carbon fiber felt: optimization of densification and carbon microstructure. Carbon 40: 2529-2545.

Zhang Weigang, Hüttinger K J. 2001. Chemical vapor infiltration of carbon – revised Part □: Model simulations. Carbon 39: 1013-1022.

ZOU Lin-hua, HUANG Yong, HUANG Po-yun and HUANG Qi-zhong. 2001. The relationship among microstructures, processing parameters and properties for carbon-carbon composites. New Carbon Materials 16(4): 63-70.